Application of Deep Learning Model to LULCC Monitoring using Remote Sensing Images

-A case study in suburban areas of central Taiwan

Presenter：Zhong-Han Zhuang / 莊忠翰

Advisor：Hui Ping Tsai / 蔡慧萍

Date：24th May, 2022

Country | Taiwan Institution | National Chung Hsing University Dept. | Civil Engineering E-mail | zhonghan.zhuang@smail.nchu.edu.tw

Outline

- Introduction
- Materials and Methods
- Results and Discussions
- Conclusion
- Future Work

Introduction

Materials and Methods

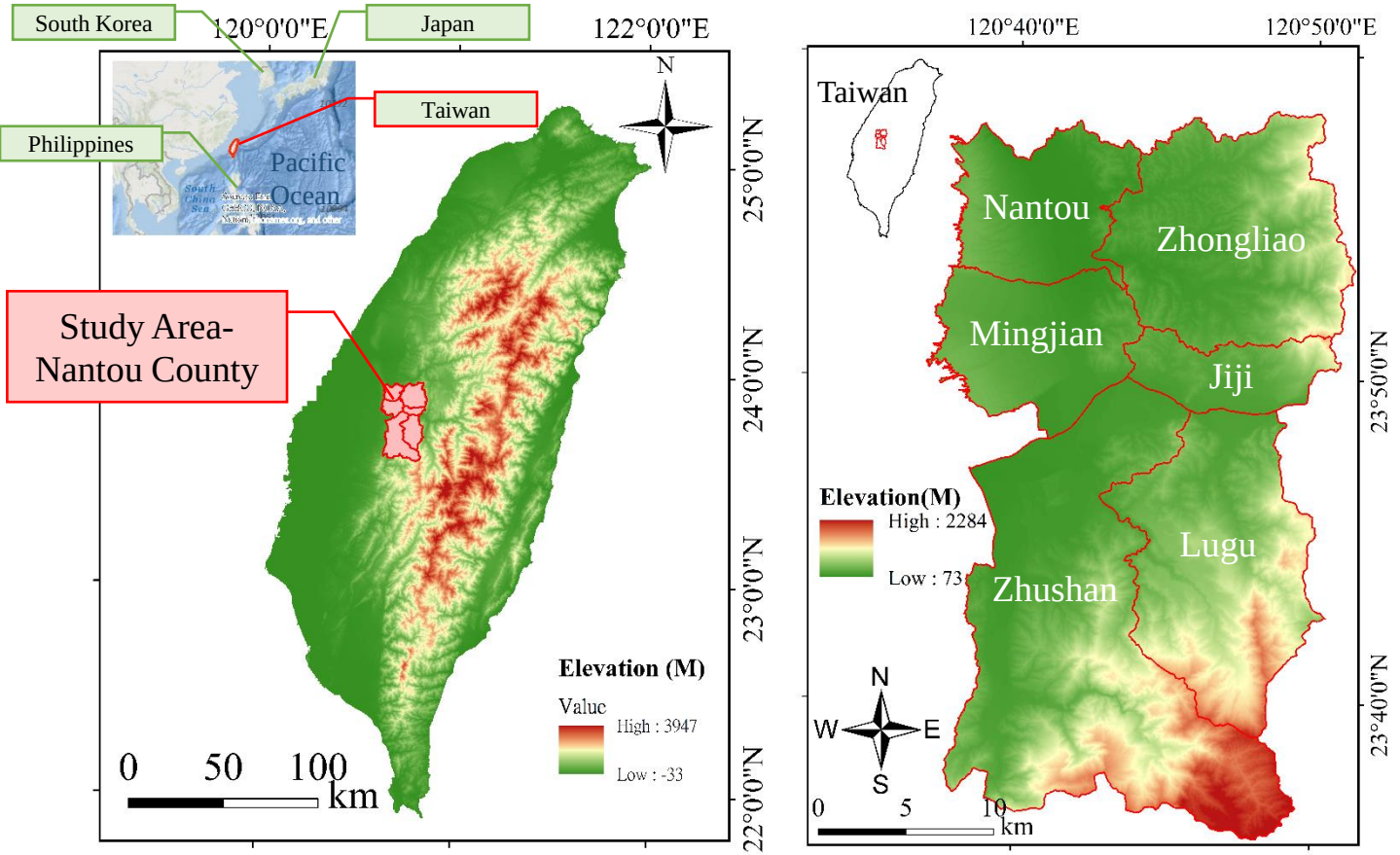

Taiwan - Located on the southeast coast of the Asian continent and the west coast of the Pacific Ocean.

Study Area-Nantou County

Area	736.4 km^2
Elevation	73 m ~ 2,284 m
Plantation	Tea、Rice、Fruits、Flowers
6 Township	Nantou City, Zhongliao, Mingjian, Jiji, Zhushan, Lugu
Land cover classes	Agriculture (Agr), Water (W), Forest (F), Bareland (BL), Built-up (BU)

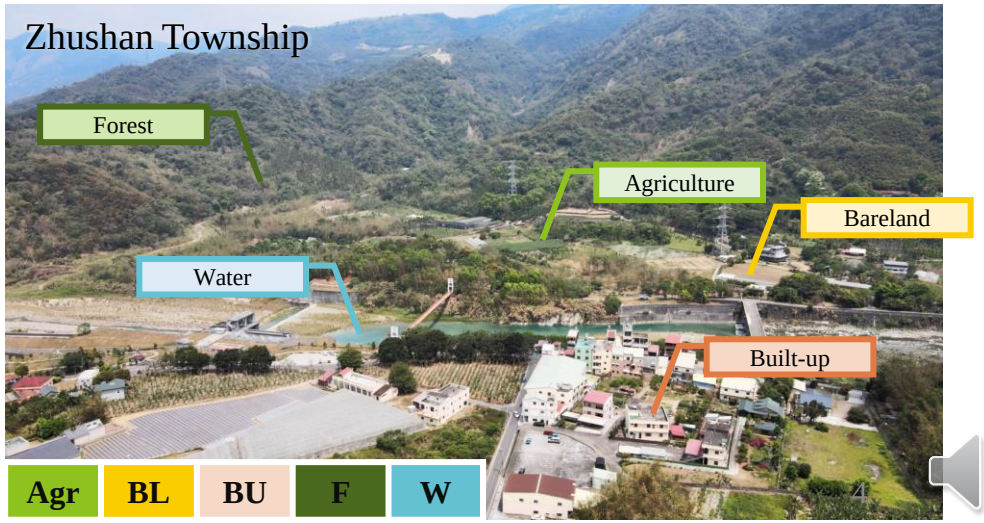

Materials and Methods

Satellite	Sentinel-2
Image Size	4302 × 3589
Resolution	10 m/pixel
Spectual Band	Blue、Green、Red、NIR
Vegetation Index	NDVI、SAVI
Acquisition Date	2018/02/15, 2019/02/15, 2020/02/25, 2021/03/16

Vegetation Index	Equation	Reference
NDVI Normalized difference vegetation index	$\frac{NIR - R}{NIR + R}$	Rouse *et al.*, 1973
SAVI Soil-adjusted vegetation index	$\frac{1.5(NIR - R)}{NIR + R + 0.5}$	Huete *et al.*, 1992

【Study Period】

【Satellite Image】

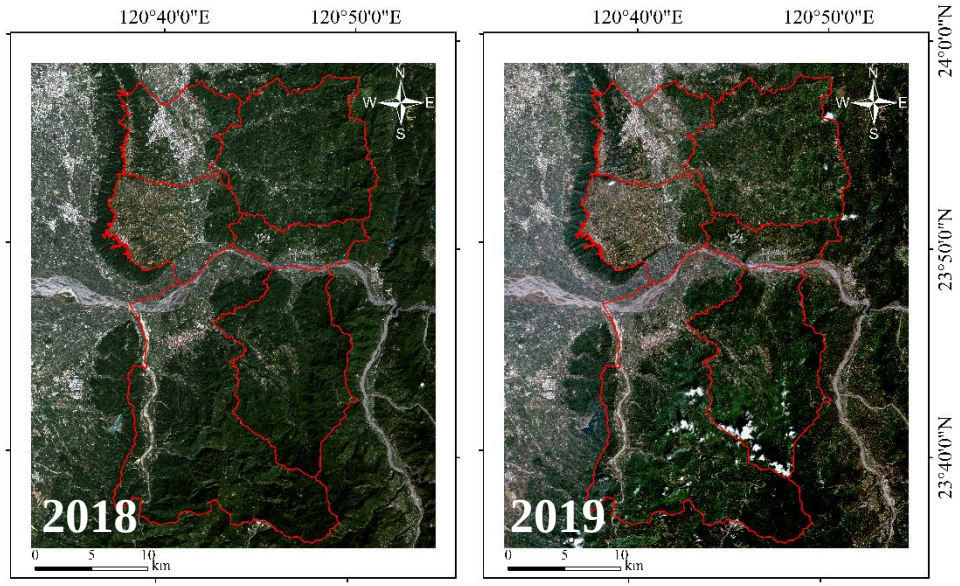

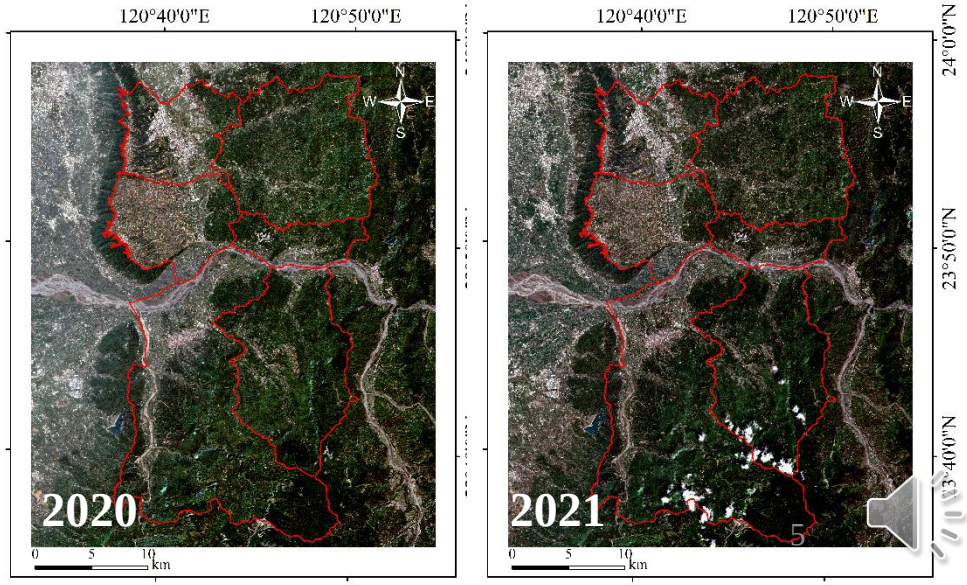

Materials and Methods

【Deep Learning Model】— U-net

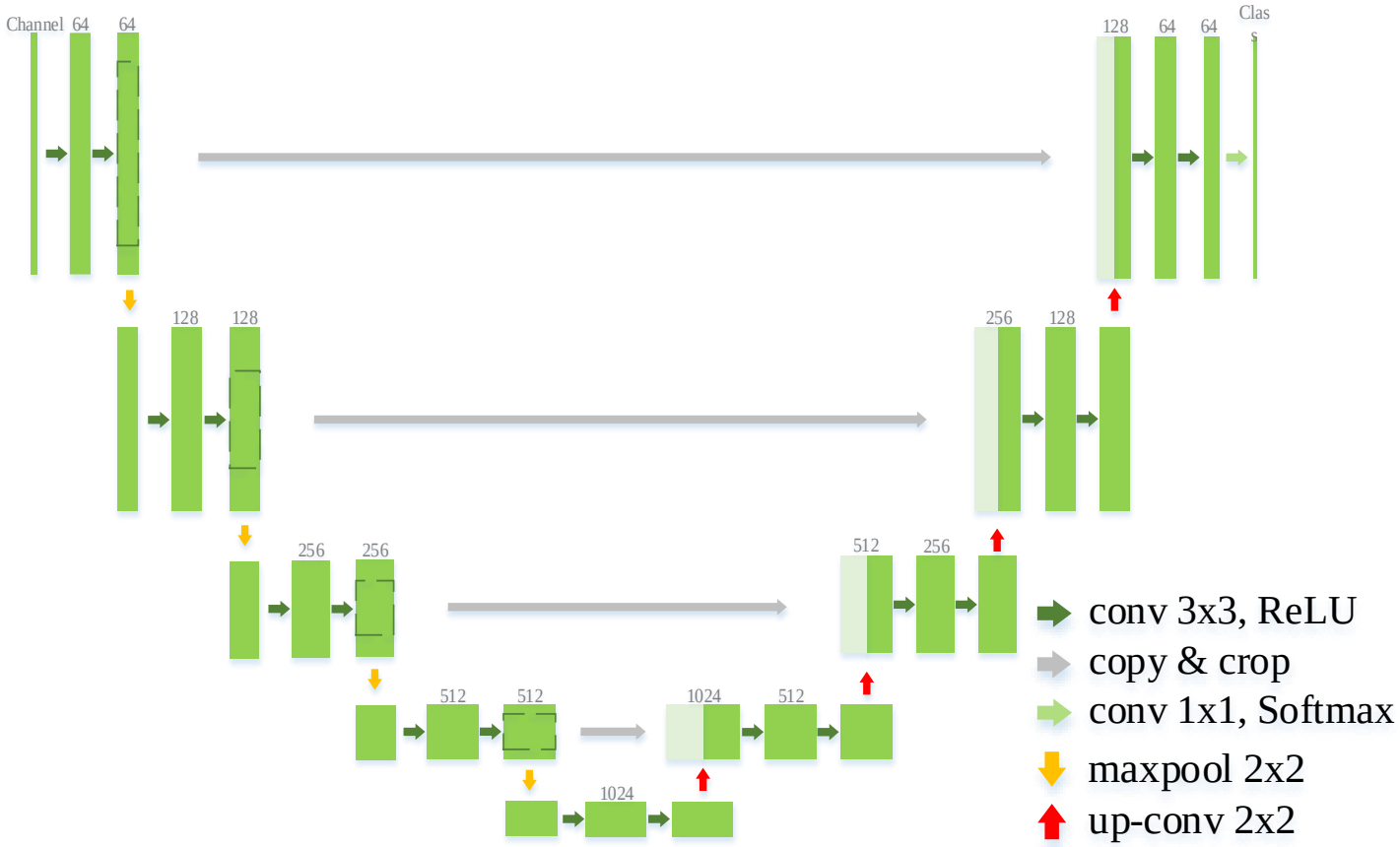

U-net Model Parameter	
Batch Size	5
No. of epochs	100
No. of training and validation images	1,250
Training image size	128 × 128
Train/Validation Ratio	8：2

Materials and Methods

【Landscape Metrics】

Landscape Metrics		
Area of each class	$\frac{Total\ Area\ in\ each\ class}{Total\ Area}$	The change trajectory of area can be measured for each class.
Number of Patches	-	The number of patches can be expressed as the degree of fragmentation of the landscape.
Mean Shape Index (MSI)	$\mathrm{SI} = \frac{0.25\sum_{k=1}^{m} e_{ik}^{*}}{\sqrt{A}}$	MSI presents the complexity of the patches, the smaller the value, the more regular the shape, means that more the intervention of human factors.
Area-Weighted Mean Patch Fractal Dimension (AWMPFD)	$\mathrm{AWMPFD} = \frac{\sum_{i=1}^{m}\sum_{j=1}^{n}\left[\frac{2\ln(0.25p_{ij})}{\ln a_{ij}}\right]}{N}$	AWMPFD is used to measure the shape and structure complexity of patches.
Shannon's Evenness Index (SHEI)	$\mathrm{SHEI} = \frac{-\sum_{i=1}^{m}(P_i \times \ln P_i)}{\ln m}$	SHEI shows the evenness of each class distribution.

Results and Discussions

【Image Classification】

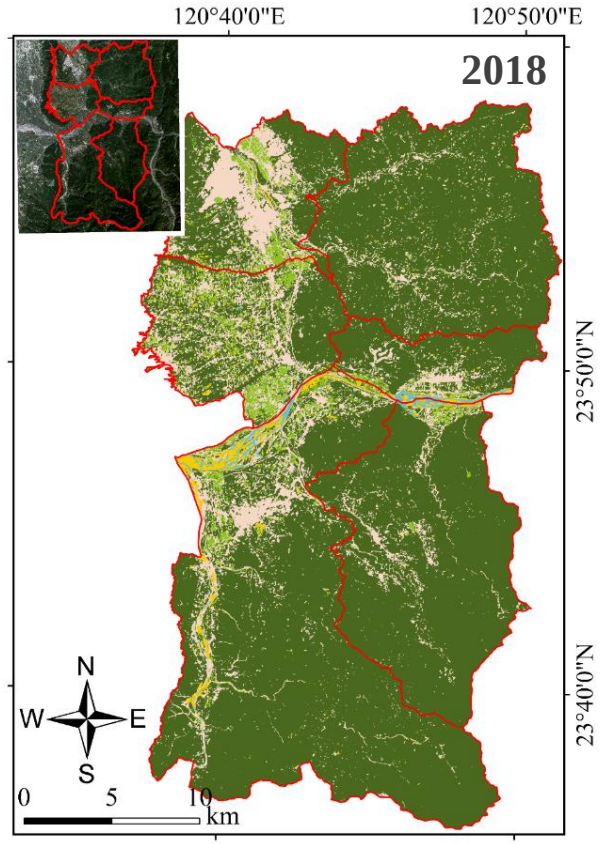

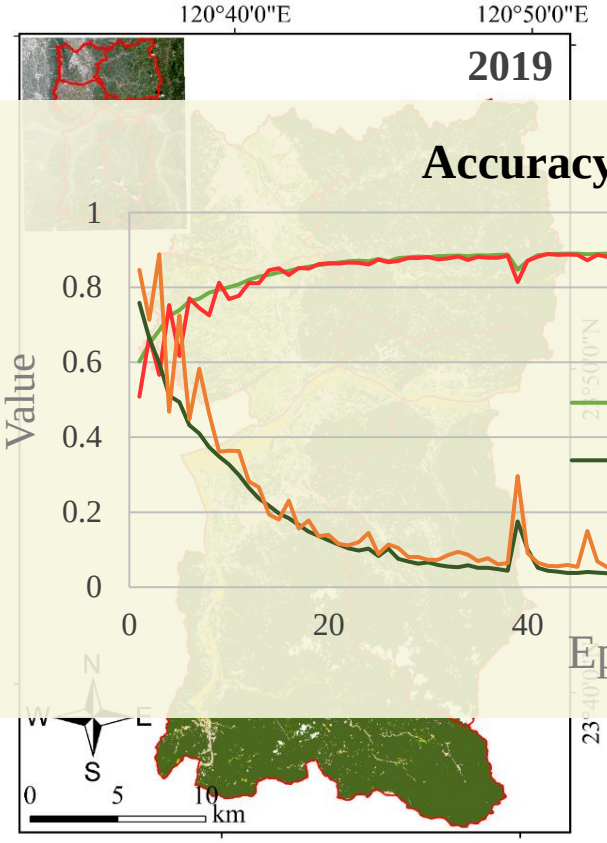

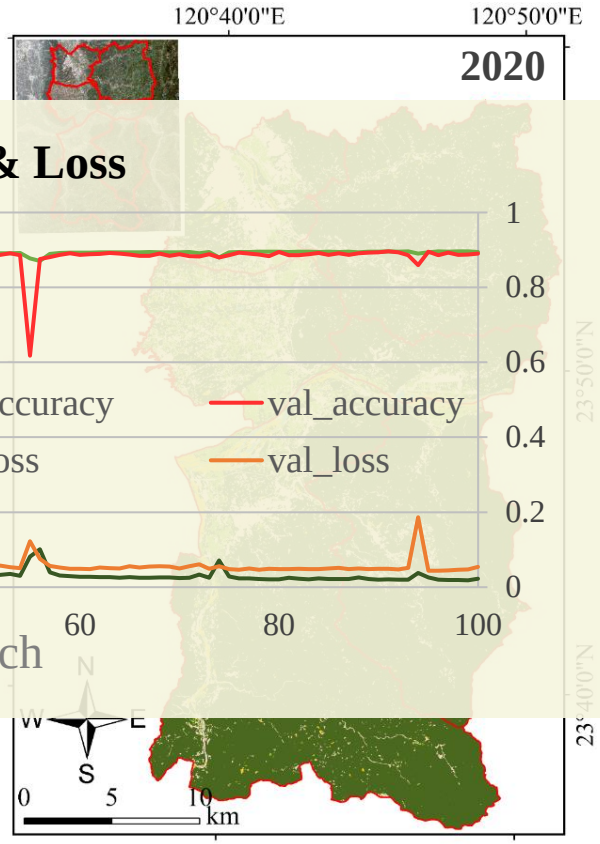

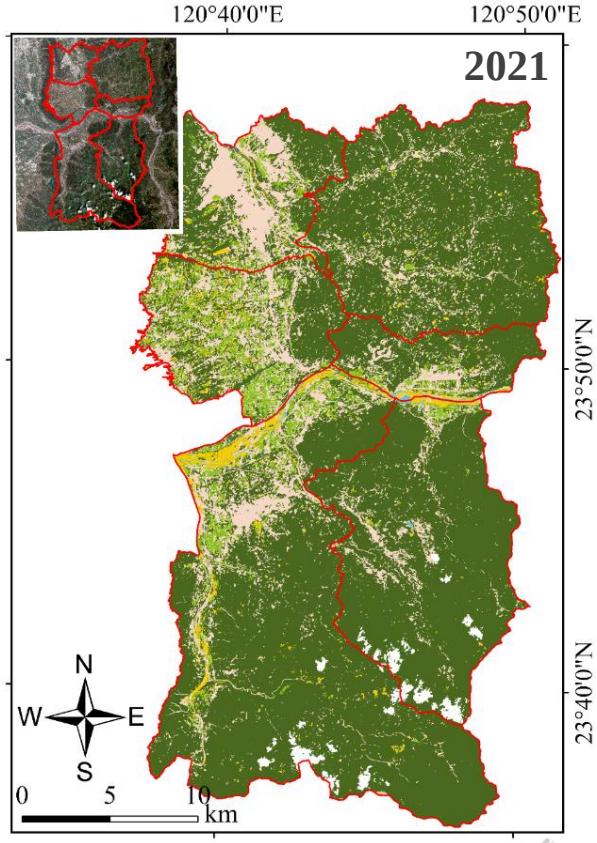

Agr BL BU F W

Results and Discussions

【Landscape】

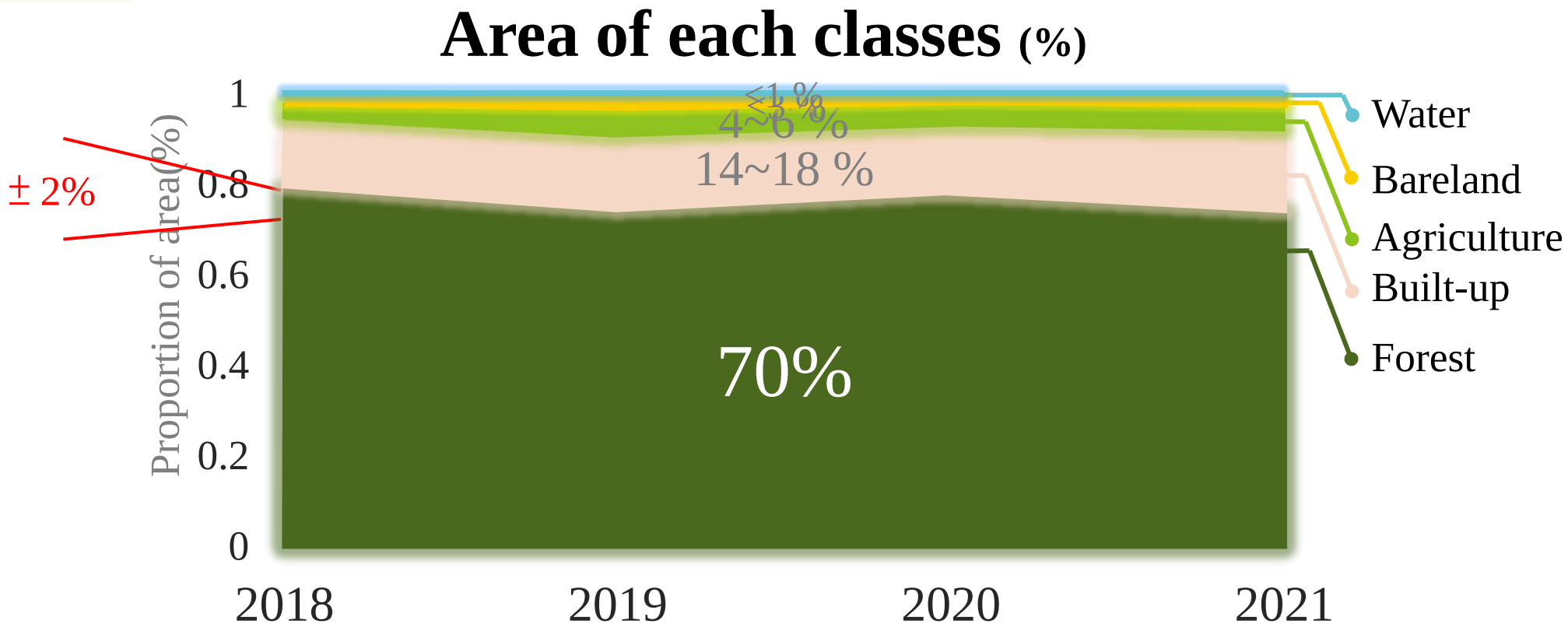

Results and Discussions

【Landscape】

Number of Patches & SHEI

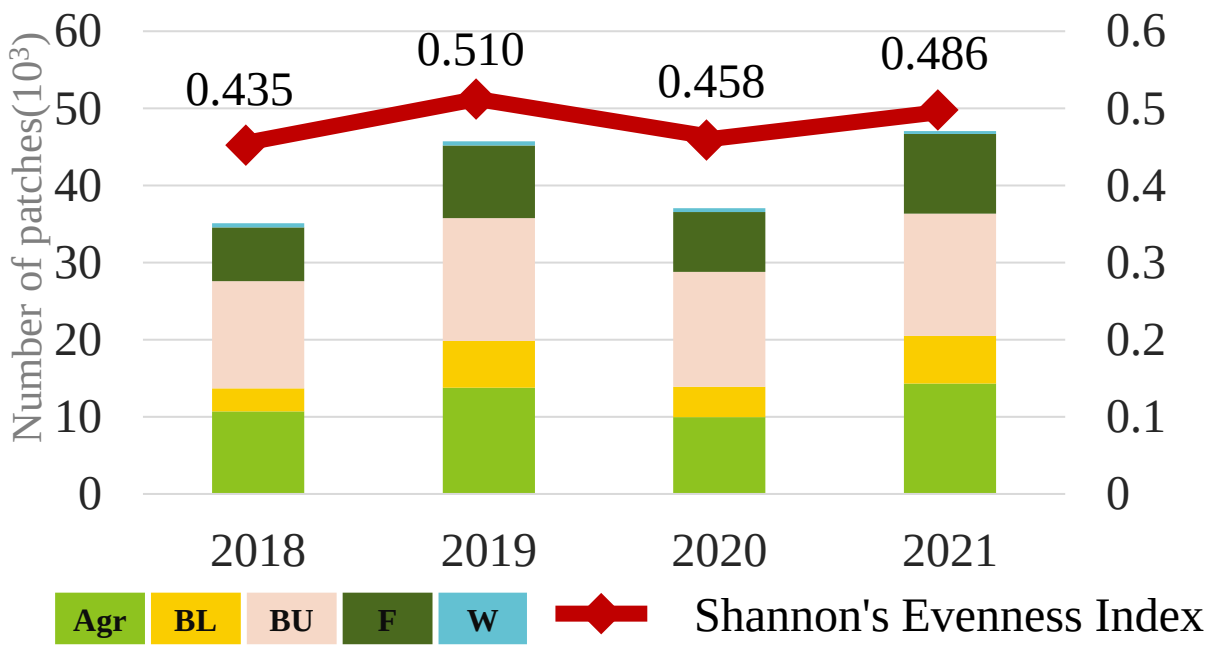

Number of Patches

Class	2018	2019	2020	2021
Agriculture	10,729	13,897	9,976	14,465
Bareland	2,985	6,258	3,929	6,417
Bulit-up	13,876	16,259	14,894	16,387
Forest	6,972	9,479	7,773	10,492
Water	558	548	485	432
# of Patches	35,120	45,721	37,057	47,084
Patch Density	39.74	52.22	41.94	54.02

Results and Discussions

【Landscape】

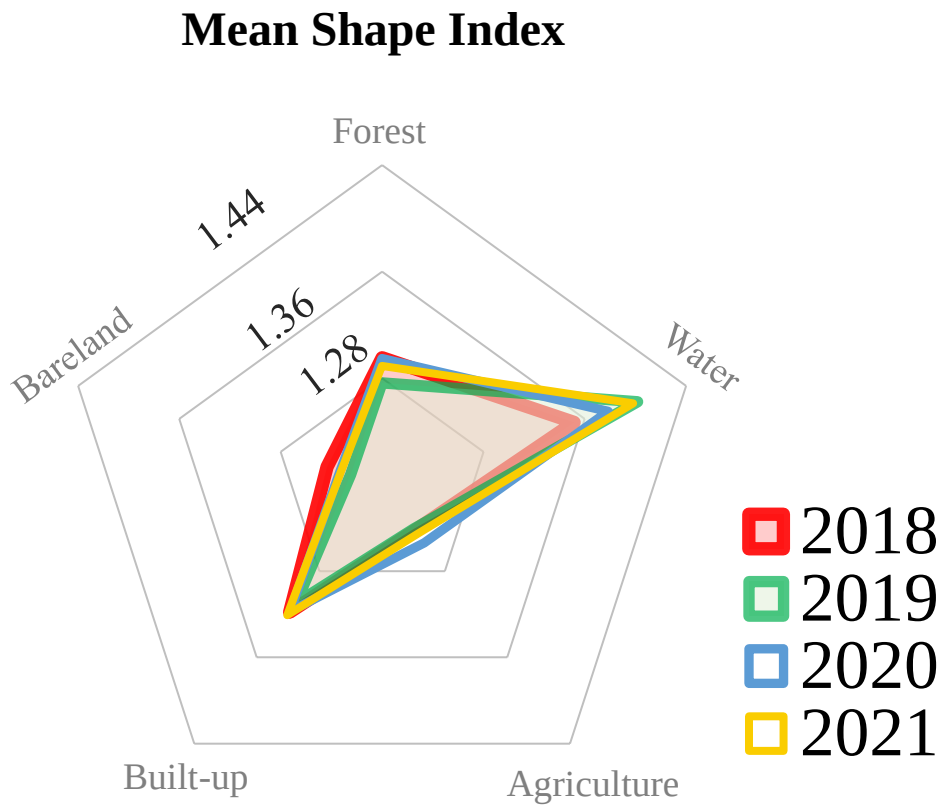

Year	Period	LSI	AWMPFD
2018	A	1.285	1.306
2019	B	1.272	1.318
2020	C	1.287	1.308
2021		1.280	1.317

LSI：Landscape Shape Index

AWMPFD：Area-Weighted Mean Patch Fractal Dimension

SHEI：Shannon's Evenness Index

Conclusion

1. The forest area has the largest area, accounting for about 70%, followed by the built-up area.
2. A slight upward trend in agricultural area.
3. The number of patches has an increasing trend in 2018-2019 and 2020-2021, indicating that there is a tendency to fragmentation.
4. The LSI and AWMPFD values show that there may be less human intervention in period 2019-2020.
5. With the change of SHEI value, the distribution of patches tends to be even except in 2019-2020.

Future Work

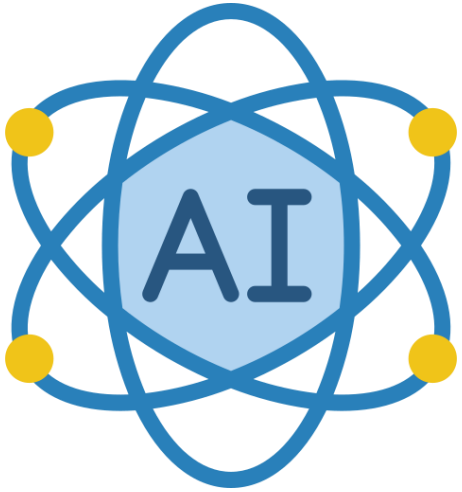

Using different classification models

Apply to others regions

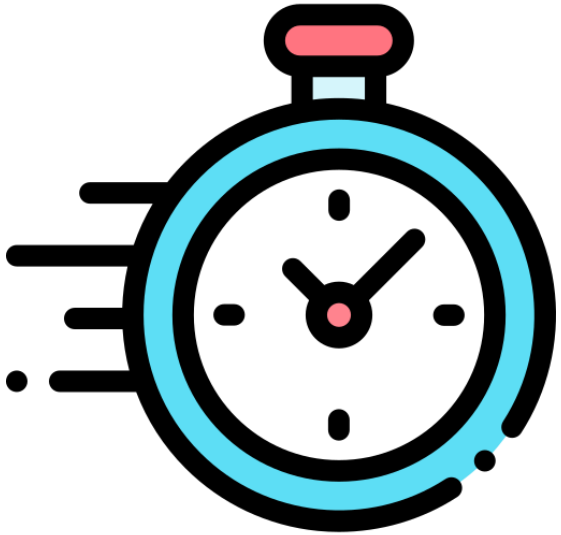

Make good use of multi-period images

References

- Ayala-Izurieta, Johanna E., et al. "Land cover classification in an ecuadorian mountain geosystem using a random forest classifier, spectral vegetation indices, and ancillary geographic data." Geosciences 7.2 (2017): 34.
- Chuang, Yung-Chung Matt, and Yi-Shiang Shiu. "A comparative analysis of machine learning with WorldView-2 pan-sharpened imagery for tea crop mapping." Sensors 16.5 (2016): 594.
- Garg, Lakshya, et al. "Land Use Land Cover Classification from Satellite Imagery using mUnet: A Modified Unet Architecture." VISIGRAPP (4: VISAPP). 2019.
- Gašparović, M., & Jogun, T., 2018. The effect of fusing Sentinel-2 bands on land-cover classification. International journal of remote sensing, 39(3), 822-841.
- Ghassemi, Sina, et al. "Learning and adapting robust features for satellite image segmentation on heterogeneous data sets." IEEE Transactions on Geoscience and Remote Sensing 57.9 (2019): 6517-6529
- Gibril, Mohamed Barakat A., et al. "Fusion of RADARSAT-2 and multispectral optical remote sensing data for LULC extraction in a tropical agricultural area." Geocarto international 32.7 (2017): 735-748.
- Huang, Yanhong, et al. "Estimating Tea Plantation Area Based on Multi-source Satellite Data." 2019 8th International Conference on Agro-Geoinformatics (Agro-Geoinformatics). IEEE, 2019.
- Huete, A. R., Hua, G., Qi, J., Chehbouni, A., & Van Leeuwen, W. J. D., 1992. Normalization of multidirectional red and NIR reflectances with the SAVI. Remote Sensing of Environment, 41(2-3), 143-154.
- Niculescu, Simona, Dino Ienco, and Jenica Hanganu. "Application of Deep Learning of Multi-Temporal SENTINEL-1 Images for the Classification of Coastal Vegetation Zone of the Danube Delta." Int. Arch. Photogramm. Remote Sens. Spat. Inf. Sci 42.3 (2018).
- Pelletier, Charlotte, et al. "Using Sentinel-2 Image Time Series to map the State of Victoria, Australia." 2019 10th International Workshop on the Analysis of Multitemporal Remote Sensing Images (MultiTemp). IEEE, 2019.
- Pelletier, Charlotte, Geoffrey I. Webb, and François Petitjean. "Temporal convolutional neural network for the classification of satellite image time series." Remote Sensing 11.5 (2019): 523.
- Ronneberger, O., Fischer, P., & Brox, T., 2015. U-net: Convolutional networks for biomedical image segmentation. In International Conference on Medical image computing and computer-assisted intervention (pp. 234-241). Springer, Cham.
- Rouse, J. W., Haas, R. H., Schell, J. A., Deering, D., Deering, W. 1973. Monitoring vegetation systems in the Great Plains with ERTS, ERTS Third Symposium, NASA SP-351 I, pp. 309-317.
- Rwanga, S. S., & Ndambuki, J. M., 2017. Accuracy assessment of land use/land cover classification using remote sensing and GIS. International Journal of Geosciences, 8(04), 611.
- Wu, Ming, et al. "Towards accurate high resolution satellite image semantic segmentation." IEEE Access 7 (2019): 55609-55619.
- Zhang, Pengbin, et al. "Urban land use and land cover classification using novel deep learning models based on high spatial resolution satellite imagery." Sensors 18.11 (2018): 3717.

EGU General Assembly 2022

Application of Deep Learning Model to LULCC Monitoring using Remote Sensing Images

-A case study in suburban areas of central Taiwan

Thank you for your attention

國立中興大學
NATIONAL CHUNG HSING UNIVERSITY

Presenter：Zhong-Han Zhuang / 莊忠翰
Advisor：Hui Ping Tsai / 蔡慧萍
E-mail：zhonghan.zhuang@smail.nchu.edu.tw

土木工程學系
Department of Civil Engineering